Physical properties of $(GaAs)_{1-x}(Ge_2)_x$: Influence of growth direction

A. G. Rodriguez, H. Navarro-Contreras, and M. A. Vidal
Instituto de Investigación en Comunicación Optica, Universidad Autónoma de San Luis Potosi, Alvaro Obregón 64, San Luis Potosi, S.L.P. 78000, Mexico

(Received 25 July 2000; revised manuscript received 01 December 2000; published 2 March 2001)

$(GaAs)_{1-x}(Ge_2)_x$ metastable alloys were epitaxially grown on (001), (111), (112), and (113) GaAs by rf magnetron sputtering. A different long-range order parameter behavior with Ge concentration is observed for each growth direction. This provides a direct evidence that growth direction affects the long-range order-disorder transition exhibited by these alloys. The epitaxial growth of these alloys was modeled by a Monte Carlo simulation. The good agreement between the experimental and modeled long-range order parameter evidences that atomic ordering in these alloys is ruled mainly by growth direction and the avoidance of the formation of ''wrong'' atomic pairs of As-As and Ga-Ga, and not by thermodynamic factors. On the other hand, measurements of the optical gap and Raman scattering, show that the optical properties are governed by near-neighbor correlations and therefore by their short-range order. Hence, the substrate orientation and the long-range order have negligible effect on the optical properties. Fitting the experimental data of the optical gap, we obtained linear expressions that show the fundamental gap behavior with Ge concentration of some of these alloys at room temperature. For $0<x<0.3$ and $0.3<x<1$ the empirical expressions are $E_0(x)=1.43-2.99x$ eV and $E_0(x)=0.45+0.35x$ eV, respectively.

DOI: 10.1103/PhysRevB.63.115328 PACS number(s): 81.15.Cd, 81.05.Ea, 64.60.Cn

I. INTRODUCTION

The metastable semiconductor alloys $(III\text{-}V)_{1-x}(IV_2)_x$, have been grown as model systems to study order-disorder transitions, where an ordered structure is associated to the zinc-blende phase (III-V-like) and the disordered structure is associated with the diamond phase (IV-like).[1–5] In these alloys a homogeneous phase is obtained at high-temperature growth (500–600 °C) only when atoms are forced to mix up to form a metastable and homogeneous phase by epitaxial techniques that operate far from thermodynamic equilibrium, otherwise if the alloys are grown by near-equilibrium-like liquid phase epitaxy or if they are exposed to sintering processes, the column-IV atoms segregate and a pronounced phase separation is observed.[6]

Since it was proposed that $(GaAs)_{1-x}(Ge_2)_x/GaAs(001)$ metastable alloys underwent a zinc-blende to diamond transition at a critical concentration $x_c(001)\approx 0.3$, because of the unusual behavior of the optical gap,[1] this and other $(III\text{-}V)_{1-x}(IV_2)_x$ metastable alloys have been the subject of several theoretical and experimental studies.[1–16] Thermodynamic and growth-kinetics models have been proposed for these alloys, looking for an explanation of the origin of the order-disorder transition.[7,10–13] Even though these models start from very different assumptions,[7,10,12] they provide information that is in good agreement with experimental data for (001)-grown alloys. The first model used to study the phase transition was performed by Dyakonov and Ralkh[15] who considered a site percolation problem of Ga and As on the diamond lattice with the restriction that no Ga-Ga or As-As nearest-neighbor pairs were allowed. This restriction is suggested by the physical fact that in order to remain transparent in the infrared region, the samples may not be permitted to become ''metallic.'' The percolation treatment led to a value of $x_c=0.57$, which is considerably higher than the experimentally observed values on samples with (001) growth direction. Another percolation model[16] also predicted an overestimated value of $x_c=0.75$. Presumably similar overestimations may be expected for the x_c values for samples grown along other crystallographic directions. The direct band gap as a function of x, was calculated using a thermodynamic model by Newman and Dow.[10] The theoretical curve, which was in reasonably good agreement with experimental data, also showed a minimum at $x=0.3$. This model had no restrictions on atomic Ga-Ga, As-As so-called ''wrong pairs.'' Later studies showed that the density of wrong pairs created by the theory should close the optical gap.[12] The absence of these wrong pairs was confirmed by x-ray-absorption fine-structure measurements.[14] Holloway and Davis (HD),[12,13] presented a kinetical model of the growth process implemented by Monte Carlo (MC) simulations, where they predicted that the long-range order-disorder transition would not be shown by (111)-grown alloys, except for pure Ge layers [i.e., $x_c(111)=1$]. Recently, we have experimentally confirmed that $(GaAs)_{1-x}(Ge_2)_x/GaAs(111)$ metastable alloys indeed do not present a long-range order-disorder transition for any Ge concentration.[9] This result strongly suggests a critical concentration dependence on the substrate orientation, which evidences an additional physical parameter influencing order-disorder transitions, namely, growth direction, to others known in the literature such as temperature, applied pressure, applied fields, etc.

We report in this work a study of optical and structural properties of $(GaAs)_{1-x}(Ge_2)_x$ metastable alloys, epitaxially grown on (001), (111), (112) and (113) GaAs. The study reveals that there is a dependence of the critical concentration on substrate orientation, that reflects on those properties that depend on the long-range ordering of the atoms, while those properties that depend only on nearest-neighboring atoms exhibit a different concentration dependence. For this purpose a long-range order (LRO) parameter behavior with

TABLE I. Time growth program of the $(GaAs)_{1-x}(Ge_2)_x$ alloys studied in this work.

Concentration, x	Targets power GaAs/Ge (W)	Time under each target GaAs/Ge (S)	Temperature (°C)	Thickness (Å)
0	50/0	1800/0	560	
0.10	30/40	3/1	550	4000
0.17	50/40	3/3	535	3800
0.18	50/40	3/3	530	3900
0.20	40/35	3/3	535	3600
0.25	40/40	3/3	535	2100
0.33	40/50	3/3	530	2700
0.40	30/50	3/3	530	2900
0.53	50/50	1/2	530	3700
0.64	30/50	2/3	520	4000
0.70	30/50	1/3	515	4500
0.78	40/50	1/4	510	3300
0.90	30/50	1/4	500	3400
1	0/50	0/1800	500	3800

Ge concentration is obtained for each growth direction. The LRO was experimentally determined by high-resolution x-ray diffraction (HRXRD) for ternary alloys semiconductors, and compared with the modeled long-range order parameters, obtained from MC simulations, which are in good agreement with experimental data, for each substrate orientation. Short-range order (SRO) is also evaluated with Raman scattering, from the ratio of TO mode to LO mode integrated intensities. In this case an almost identical behavior is observed for differently oriented grown alloys. We also present measurements of the optical gap for these alloys. All sets of alloys show an almost identical fundamental gap behavior with Ge concentration, which further exhibits that the SRO is independent of the substrate orientation and that the long-range zinc-blende to diamond transition has negligible effect on the fundamental gap.

II. EXPERIMENTAL PROCEDURES

$(GaAs)_{1-x}(Ge_2)_x$ metastable alloys were epitaxially grown on (001), (111), (112), and (113) GaAs, in a rf planar magnetron sputtering system with a base pressure better than 10^{-7} mbar. Two independent Ar (99.999%) glow discharges were maintained to pulverize two 10-cm, water-cooled Ge (99.999%) and GaAs (99.999%) targets at a sputtering pressure of 2×10^{-2} mbar. For each experiment 1×1 cm^2 epiready semi-insulating GaAs wafers of the four orientations were In-glued to a molybdenum block, which was introduced into the system through a load chamber. The substrate holder was placed 2 mm above a BN heater, with target-substrate separation of 5 cm. The growth conditions are summarized in Table I.

The growth base pressure (10^{-7} mbar) is relatively high and therefore carbon and oxygen should be present in our samples. However, our results (lattice parameter, LRO parameter, and optical band gap) on (001) GaAs growths give very similar data to that obtained in samples grown by molecular beam epitaxy (MBE)[8] and metal-organic chemical-vapor deposition (MOCVD).[3] This strongly suggests that oxygen, carbon, and any other impurities are unimportant for the physical properties discussed in this paper.

All samples were measured by HRXRD in a MRD Philips diffractometer. The integrated intensities, peak positions, and the full width at half maximum (FWHM) of the rocking curves were determined by least squares fits to Gaussian line shapes.

Raman scattering experiments were realized at room temperature in the $z(xy)\tilde{z}$ backscattering geometry using a Jobin-Yvon T 64 000 spectrometer with the 5145-Å line of an Ar laser and a charge coupled device detector.

Optical fundamental gaps were obtained from absorption spectra at room temperature using a spectrophotometer Cary 5E. The samples were mechanically polished in order to remove the In used to glue the substrates during the growth process. In order to perform a substrate correction during the measurements, a substrate with the same characteristics of those of the samples was placed in the reference beam.

The photoreflectance (PR) of all the samples was measured in a system consisting of a 0.5-m SCIENCETECH 9040 monochromator. The light of a tungsten lamp dispersed by the monochromator was used as the probe beam. The 6328-Å line of a He-Ne laser chopped at 100 Hz provided the optical modulation.

III. LONG-RANGE ORDER PARAMETER DETERMINATION

The long-range atomic order parameter S, for $(III\text{-}V)_{1-x}(IV_2)_x$ alloys is given by $S(x)=2r(x)-1$,[2] where r is the probability that any given Ga (or As) atom will occupy its site in the lattice. For a disordered crystal, $r=0.5$, while for perfect long-range order $r=1$.

Long-range order parameter as a function of Ge concentration, was determined for each growth direction following the procedure given by Shah *et al.*[2] Different diffraction profiles obtained by HRXRD are required in order to analyze the zinc-blende to diamond transition. For this purpose it is necessary to compare the integrated intensities of fundamental and superstructure reflections.[2,17] Reflections that are allowed for both zinc-blende and diamond structures are called fundamental, while superstructure reflections are those only exhibited by a zinc-blende structure.[17] The choice of reflections used in this work was made from those that could be measured in our diffractometer for each substrate orientation.

The ratio R, of the superstructure to fundamental reflection integrated intensities of the alloy, normalized to those of the substrate is given by[2]

$$R=\frac{[I_{\text{superstructure}}/I_{\text{fundamental}}]_{\text{alloy}}}{[I_{\text{superstructure}}/I_{\text{fundamental}}]_{\text{substrate}}}.$$

As the integrated intensity directly depends on the structure factor, and this on atomic scattering factors, it is necessary to evaluate the scattering factors at the diffraction angle corresponding to the different reflections for each substrate orientation. Given the similarity in atomic scattering factors of

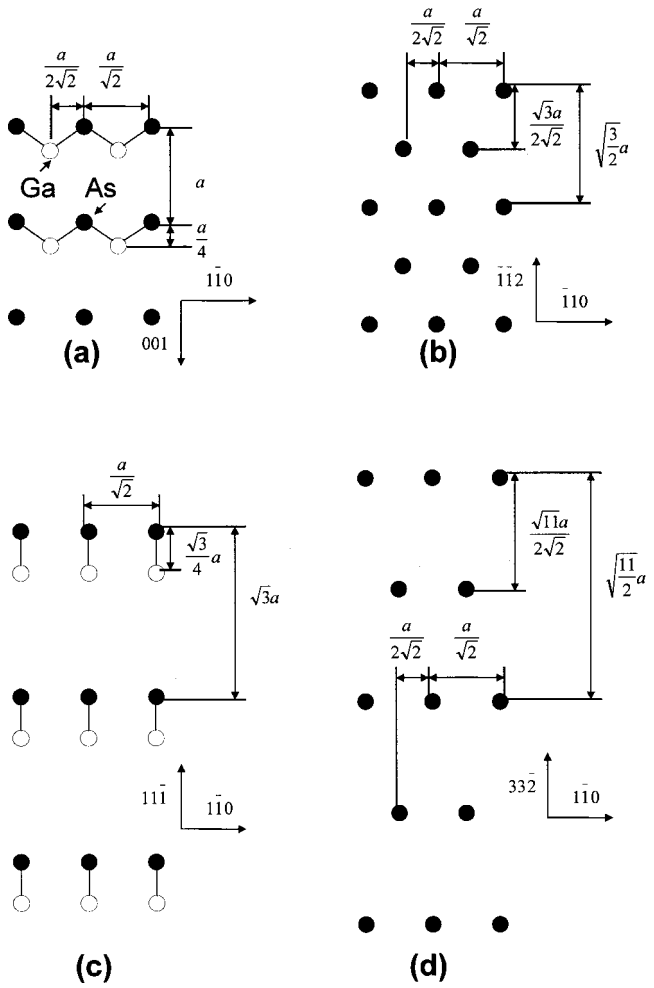

FIG. 1. Distribution of the atoms on surface parallel planes for different GaAs substrate orientations, (a) (110), (b) (111), (c) (112), (d) (113). The full circles represent As atoms, and the position of Ga atoms is marked by open circles. All the atoms shown are in the same plane for each substrate orientation. The arrows in the figure give the directions orthogonal to the surface for each orientation. The distances between the atoms are marked in the figure as a function of the lattice constant (a).

Ga, Ge, and As, S can be taken as $S=R^{1/2}/(1-x)$ for the full range of atom-IV concentrations, for all the studied substrate orientations.[2]

IV. MONTE CARLO GROWTH MODEL

The epitaxial growth of $(GaAs)_{1-x}(Ge_2)_x$ on (001), (110), (111), (112), and (113) GaAs, was simulated using a Monte Carlo model. This model assumes a stochastic growth process to choose the atomic positions and atom type. The effect of substrate orientation is considered by taking account the different geometrical relationships between atoms in the planes for each growth direction.[12,13]

Growth initiates on a surface-parallel crystal plane of a GaAs substrate. For the growth directions (001), (111), and (113), the occupancy of successive planes alternates between all Ga and all As atoms (Fig. 1). On the other hand, (110) and (112) planes are occupied by both Ga and As atoms. The growth simulation was carried out layer by layer. Only Ga and Ge are chosen at random to fill an empty site also chosen at random in a given plane.[12,13] A Ge atom is added with the probability P, while the incorporation of a Ga atom is subject to the probability $(1-P)$. Because an As excess is supposed to exist during the crystal growth, every time a Ga atom is added, an As atom immediately takes a nearest-neighbor (NN) position in one of the following planes. A Ga atom is only incorporated if it does not create Ga-Ga or As-As NN ''wrong'' pairs; if these pairs are produced, a Ge atom is placed instead. It is considered that every unwanted Ga evaporates immediately. Although the model is not entirely realistic, as several physical factors are not incorporated by it (such as surface diffusion process of the arriving atoms, terrace formation during the growth, impurities incorporation, etc.), the model as we discuss below provides an excellent prediction of the LRO parameter behavior with Ge concentration for the different substrate oriented growths, that we feel it justifies our use of it to get a physical picture of the most important physical parameters that determine the growth process.

Modeling was carried out using planes of 50×50 atoms along directions orthogonal to the substrate orientation (Fig. 1), up to 20 000 atomic planes. The use of larger planes was found to have insignificant effects in our results. It was supposed that the sample was periodic across the orthogonal boundaries for all the substrate orientations.

The long-range order parameter M, can be defined as a function of an antisite fraction f, as $M=(1-x)(1-2f)=(1-x)S$,[13] where $f=1-r$ is the fraction of Ga (As) atoms that are in the As (Ga) sites, with respect to the substrate over which simulated growths are carried out. This f, takes values from zero (zinc-blende structure) to 0.5 (diamond structure). It is also convenient to define the phase and antiphase orientations. The phase orientation of GaAs is that which has its Ga and As atoms, following the same atomic arrangement of the GaAs substrate. On the other hand, f is the fraction of GaAs that is in the antiphase orientation.

A variable that reflects the size of the domains of Ge and GaAs in the growth direction, is the mean cluster length $\langle l\rangle$.[13] The length $\langle l\rangle$ is defined as the number of atoms of the same component that can be reached from an atom going to preceding planes through NN bonds. Understanding by a component either GaAs in phase, GaAs in antiphase, or Ge. For each component, $\langle l\rangle$ is the average of l over all atoms of the same kind within the sample. For instance, in a perfect GaAs crystal $\langle l\rangle_{\text{phase}}$ is a very large number (tends to infinity) and $\langle l\rangle_{\text{antiphase}}$ is zero (there are not antisite defects). The trips through NN bonds were restricted to those that might be done to preceding planes or in the same plane [for (110) and (112) alloys]. Traveling by a combination of backward and forward moves was not allowed.

The results of the simulated epitaxial growth are presented for each growth direction. We also present a prediction of the long range order parameter behavior for (110)-grown alloys.

The reciprocal of the mean cluster length of each component are shown in Figs. 2 and 3. We observe that our results for (001)-grown alloys reproduce those previously reported

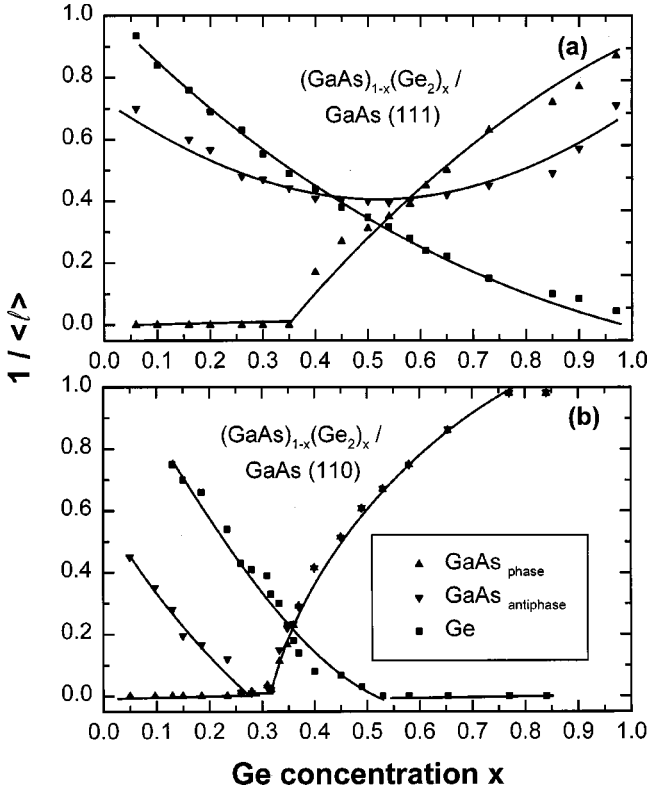

FIG. 2. Mean cluster lengths reciprocal ($1/\langle l\rangle$) from Monte Carlo simulations for (a) (111) and (b) (110) alloys. The lines are for visual aid only. Full up (down) triangles show the behavior with Ge concentration for the GaAs phase (antiphase) component. The full squares give the domain size for the Ge component.

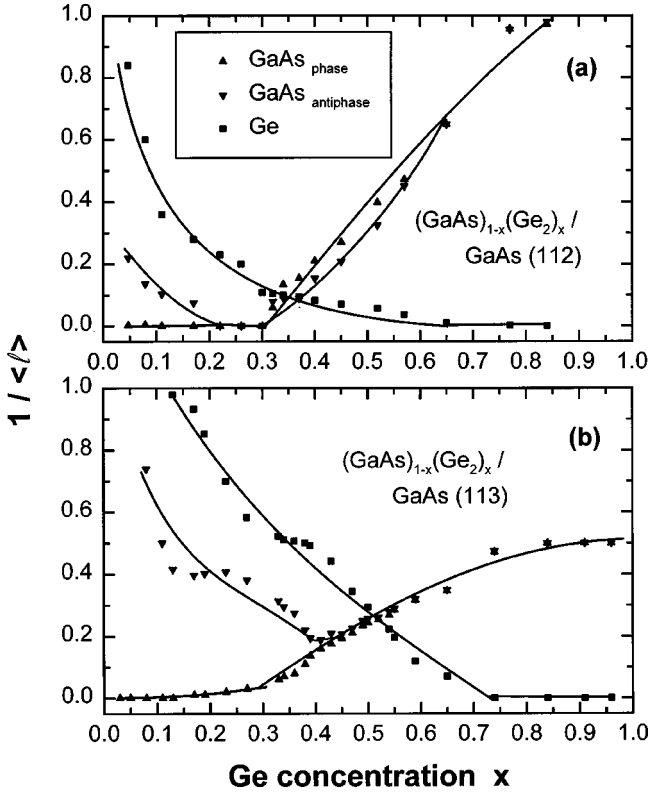

FIG. 3. Simulated average cluster reciprocal lengths for (a) (112) and (b) (113) alloys. Full up (down) triangles show the behavior with Ge concentration for the GaAs phase (antiphase) component. The full squares give the domain size for the Ge component. The lines joining the points are shown for visual aid only.

by HD (Ref. 12) and will not be not discussed here.

The modeled domain size for (111)-grown alloys is given in Fig. 2(a). The obtained phase and antiphase domain sizes reproduce those previously reported by HD.[13] Even for high Ge concentrations there is always a difference in the mean cluster length of phase and antiphase GaAs, in a large volume average there is a dominant GaAs atomic arrangement, i.e., long-range order is retained in the whole compositional range for (111) alloys. We obtained a different behavior of the Ge component to that presented by HD,[13] in their simulations the Ge component acquires infinite length for $x \geqslant 0.61$, in this work however, this component does not reach an infinite length for any $x<1$, which is a more expectable result if the alloy does not suffer a long-range order-disorder transition. The LRO parameter obtained from the simulation for (111) alloys is shown in Fig. 4(a) with a dashed line.

We also present a prediction for the long-range order in (110)-grown alloys. The modeled domain size for alloys grown with this orientation is shown in Fig. 2(b). The GaAs phase component has an infinite extent for Ge concentrations below 0.30, and a finite length above this value. The GaAs antiphase component reaches an infinite domain size in the compositional range between 0.26 and 0.30 and has a finite size for other compositions. Phase and antiphase GaAs have the same average length for $x \geqslant 0.40$. The mean cluster length of the Ge component becomes infinite for concentrations larger than 0.51. The critical concentration obtained is $x_{cMC}(110) \cong 0.4$.

In Fig. 3(a) the behavior with Ge concentration for $1/\langle l\rangle$ is presented for (112)-grown alloys. For $x \leqslant 0.21$ there is an infinite GaAs (phase) domain and both the GaAs antiphase and Ge components domains increase their size with Ge concentration. The antiphase GaAs presents an infinite length in $0.21 \leqslant x \leqslant 0.3$. In this range the phase GaAs remains infinite and the Ge component finite. Both GaAs phase and antiphase components acquire a finite domain size for compositions larger than 0.30, a fact that is also reflected with a slope change of the Ge component at $x=0.30$. For $x \geqslant 0.63$ the Ge cluster length become infinite and the phase and antiphase components of GaAs have the same average size for compositions larger than 0.65. The LRO parameter behavior with Ge concentration for (112)-grown alloys is shown with a dashed line in Fig. 4(b). A slower decrease in order parameter with respect to (001)-grown alloys is observed in the calculated parameter. A critical concentration, characteristic of this substrate orientation is obtained by the simulations $x_{cMC}(112)=0.65$.

For (113)-grown alloys the average reciprocal cluster length is shown in Fig. 3(b). The GaAs phase component has an infinite cluster size for compositions under 0.21, for Ge concentrations larger than this value this component has a finite size. As for (111) alloys, the GaAs antiphase component never reaches an infinite length in the compositional

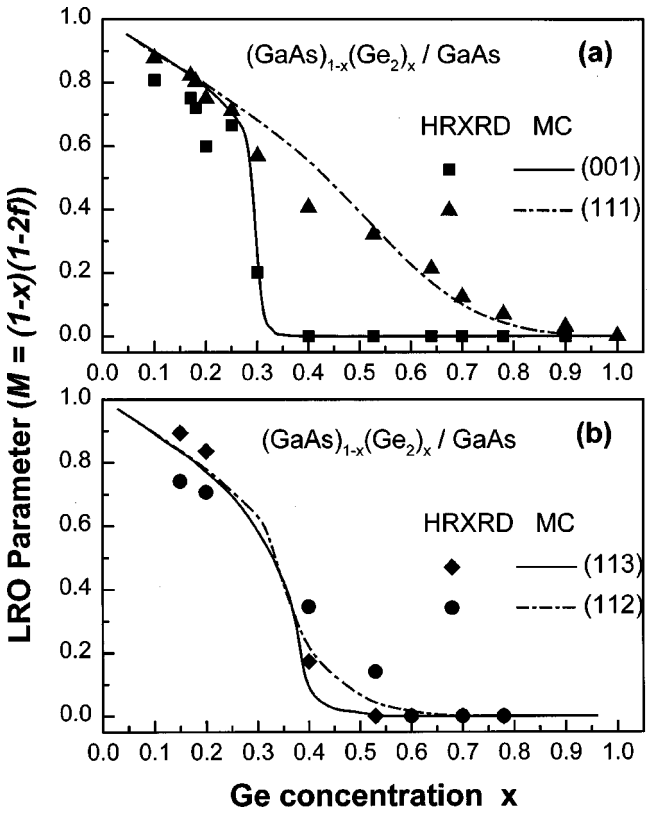

FIG. 4. Experimental and modeled long-range order parameter behavior with Ge concentration of $(GaAs)_{1-x}(Ge_2)_x$ epitaxially grown on (a) (001) and (111) and (b) (113) and (112) GaAs. This figure clearly shows the influence of growth direction on the order-disorder transition exhibited by $(GaAs)_{1-x}(Ge_2)_x$ metastable alloys.

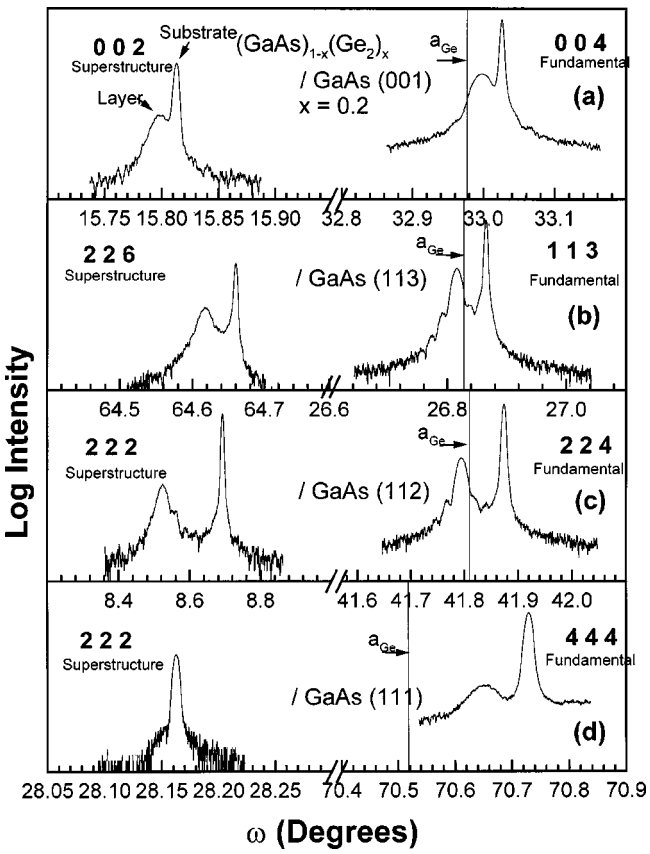

FIG. 5. Typical diffraction profiles of fundamental and superstructure reflections obtained by HRXRD for $(GaAs)_{0.8}(Ge_2)_{0.2}$ metastable alloys epitaxially grown on (a) (001), (b) (113), (c) (112), and (d) (111) GaAs. The superstructure peak associated with the alloy is present in all the differently oriented layers, this means that at this Ge concentration all the layers have a zinc-blende structure.

range, however the mean cluster sizes for the phase and antiphase GaAs become equal for compositions above 0.54, so there is not a predominant GaAs arrangement and the crystal suffers a zinc-blende to diamond transition. For $x \geqslant 0.72$ there is an infinite Ge domain. The solid line in Fig. 4(b) shows the behavior with Ge concentration of the LRO parameter for (113)-grown alloys. The critical concentration obtained from the simulation for alloys grown with this orientation is $x_{c\mathrm{MC}}(113) = 0.54$.

V. EXPERIMENTAL RESULTS AND DISCUSSION

A. High resolution x-ray diffraction

Typical diffraction profiles of fundamental and superstructure reflections of $(GaAs)_{1-x}(Ge_2)_x$ metastable alloys are shown in Figs. 5 and 6 for each growth direction for Ge concentrations $x = 0.2$ and $x = 0.7$, respectively. Superstructure reflections rocking curves are shown at the left of these figures while fundamental reflections are placed at the right side. For all the substrate orientations the peaks of the layer and substrate are clearly observed in the fundamental reflections exhibiting the epitaxial growth of our films. The angular peak separation of the layer and substrate increases with Ge concentration. The vertical solid lines shown in the fundamental reflections indicate the Bragg peak positions for a Ge layer pseudomorphically grown on GaAs. It has been previously observed that bulk lattice parameter behavior with Ge concentration of these alloys, does not follow Vegard's rule.[3,5,8] Reported values for lattice parameter are always larger than those expected from a linear interpolation between GaAs and Ge bulk lattice parameters.[3,5,8]

From the asymmetrical reflections 224 and 115, we know that our (001) films are pseudomorphically grown on GaAs. From simulations of diffraction profiles for other crystalline orientations, using the same parameters (Ge composition and thickness) of (001) alloys by dynamical theory and comparing them with experimental rocking curves of the other simultaneously grown alloys for each Ge concentration, we know that the (111)-, (112)-, and (113)-grown alloys are also coherently strained. Angular separations between the layer and substrate peaks become larger than those marked by the vertical lines at a given Ge concentration, this exhibit the deviation from Vegard's rule mentioned above. FWHM of the layer peaks are larger than that of the substrate. This FWHM is mainly determined by the layer thickness along the growth direction. FWHM corrected for layer thickness are between 0.004° and 0.009°, which are of the same order of the FWHM of the substrate. This fact together with the

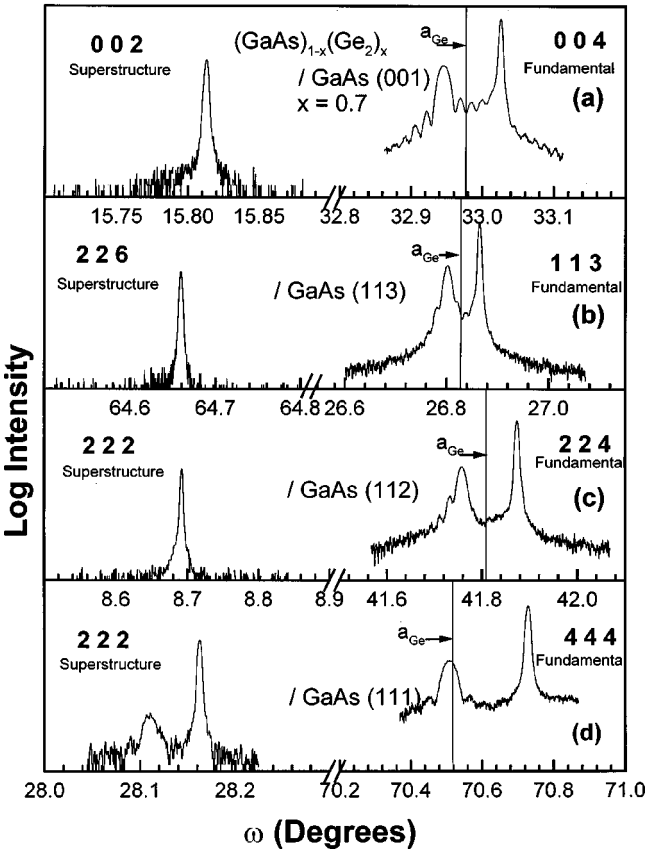

FIG. 6. Fundamental and superstructure reflections rocking curves of $(GaAs)_{0.3}(Ge_2)_{0.7}$ epitaxially grown on (a) (001), (b) (113), (c) (112), and (d) (111) GaAs. The superstructure peak associated with the alloy has vanished for all growth directions except for the (111)-grown alloy. Only the (111)-oriented layer has a zinc-blende structure at this Ge concentration.

observation of Pendellösung fringes exhibits the high structural quality of our films. The interference fringes, also allowed us to determine the layer thickness from HRXRD.

Figure 5 shows the typical fundamental and superstructure reflections for $x=0.2$ alloys. As can be seen in this figure, the layer peak of the superstructure and fundamental reflections is present in all the diffraction profiles indicating that all the differently oriented alloys have the zinc-blende structure for this Ge concentration. Alloys with $x=0.7$ are presented in Fig. 6. The layer peak in the superstructure reflections has already vanished for all the substrate orientations except the (111)-grown alloy. For (111)-grown crystals the layer peak does not disappear for any superstructure reflection, but it is present even in samples with high Ge concentration. This fact is an evidence that when $(GaAs)_{1-x}(Ge_2)_x$ metastable alloys are grown on (111) GaAs substrates, they retain long-range order throughout the full compositional range. The long-range order parameter behavior with Ge concentration for (111) grown alloys is shown in Fig. 4(a) with full triangles. We can observe that these layers do not show a zinc-blende to diamond transition for any Ge concentration.

For (001)-grown alloys, the superstructure layer peak vanishes when Ge concentration is increased, evidencing an order-disorder transition at $x_c(001)\approx 0.36\pm 0.04$. The uncertainty is derived from the fit to the experimental points added to that of the uncertainty in the alloy Ge concentration determination ($\approx$1% by itself). The long-range order parameter behavior with Ge concentration, obtained from HRXRD rocking curves, is shown in Fig. 4(a) in full squares. Experimental results are in good agreement with previously reported data for this alloy and other $(III-V)_{1-x}(IV_2)_x$ metastable alloys also obtained by HRXRD, $x_c(001)\approx 0.34$ for $(GaAs)_{1-x}(Ge_2)_x$ (Ref. 5) and $x_c(001)\geqslant 0.30$ for $(GaSb)_{1-x}(Ge_2)_x$.[2] And with values obtained from other techniques $x_c(001)\approx 0.34$ for $(GaAs)_{1-x}(Si_2)_x$ (Ref. 18) from differential reflectance spectroscopy.

TABLE II. Comparison between critical Ge concentrations at which the zinc-blende to diamond transition of $(GaAs)_{1-x}(Ge_2)_x$ alloys occurs.

Growth direction	x_c (HRXRD)	x_c (MC)
(001)	0.36 ± 0.04	0.33
(110)		0.40
(113)	0.50 ± 0.04	0.54
(112)	0.59 ± 0.04	0.65
(111)	0.96 ± 0.04	1.0

For (112)-grown alloys, we can see that the alloy peak in the superstructure reflections also vanishes within the compositional range studied. However, the alloy does not change to the higher symmetry structure at the same Ge concentration that (001) alloys do. That is, although (112)-grown alloys do show a zinc-blende to diamond transition, the critical concentration is not the same that is observed for (001) alloys. Figure 4(b) shows the experimental data for the long range order parameter of (112) alloys in full circles. The order-disorder transition is shown at $x_c(112)\approx 0.59\pm 0.04$.

From Fig. 6, it is clear that alloys grown with the substrate orientation (113) also suffer a zinc-blende to diamond transition. However, now the critical concentration experimentally obtained is neither that of (001) or (112) alloys. The long-range order parameter for different Ge concentration of these alloys is shown in Fig. 4(b) in full diamonds. The critical concentration for this orientation is found to be $x_c(113)\approx 0.50\pm 0.04$.

From the comparison of the experimental and modeled long-range order parameter for the different growth directions presented in Fig. 4, we can see that there is a good agreement between both kind of parameters for all substrate orientations considered. It is evident that long range atomic ordering in these alloys is ruled mainly by the substrate geometry. The main features of the modeled LRO parameter behavior with Ge concentration are exhibited by the experimental data and the critical concentrations obtained from the experiment compare well with those obtained from the simulations. The different critical concentrations obtained for each growth direction from the experiments and modeling are summarized in Table II.

As mentioned in the introductory remarks, several thermodynamic and growth kinetics models have been proposed

for these alloys, looking for an explanation of the origin of the order-disorder transition.[7,10–13] The so-called thermodynamical models minimize the Helmholtz free energy that is determined by assuming some kind of arrangement of atoms with probability considerations as to which position in the lattice the different Ga, As, and Ge atoms may occupy. Even though these models start from very different assumptions,[7,10,12] they provide information that is in agreement with experimental data for the critical value of the concentration at which the order-disorder transition takes place, and among themselves *but only* for (001)-grown alloys.[1,7,10] None of them predict *any different* x_c for samples grown on different oriented substrates. Our results clearly rule out the applicability of these models to the experimental data presented in this work. Our results of the Monte Carlo simulation of the epitaxial growth of these alloys for (001)-, (111)-, (112)-, (113)-, and (110)-oriented substrates, and their good agreement with the experimentally observed long-range order parameter indicates that the atomic ordering in these alloys is in reality ruled mainly by growth direction and the prohibition to form wrong Ga-Ga and As-As pairs. This fact is strengthened by the fact that for the similar alloys $(GaSb)_{1-x}(Ge_2)_x$ and $(GaAs)_{1-x}(Si_2)_x$, but of different composing atoms grown on top of (001) substrates, a similar critical concentration $x_c \approx 0.3$ is obtained.

A point to remark is that the deviation of Vegard's law and order-disorder transition at $x_c \cong 0.3$ of (001)-direction growth are also observed in layers grown by MBE (Ref. 8) and MOCVD,[3] therefore growth unintended effects such as surface damage or impurity atoms diluted into the samples cannot be responsible of Vegard's law deviation or of the order-disorder transition.

B. Raman scattering

The Raman spectra for (001), (111), (112), and (113) are very similar. Short-range order can be evaluated using the ratio of TO mode to LO mode integrated intensities (I_{TO}/I_{LO}).[19,20] The asymmetrical line shape of the experimental spectra was fitted to a Lorentzian times an exponential decay function for each optical phonon,[20] so peak positions, FWHM and integrated intensities could be obtained. The behavior with Ge concentration of the ratio I_{TO}/I_{LO} is shown in Fig. 7 for the four crystalline orientations. The dashed lines are shown for visual aid only. The values of the ratio I_{TO}/I_{LO} are very similar for the differently oriented grown alloys. For all samples, except those grown on (001) substrates, the alloy I_{TO}/I_{LO} ratios are divided by the correspondent pure GaAs ratio determined from a similarly oriented clean substrate. The ratio I_{TO}/I_{LO} increases with Ge concentration for $x<0.2$ because the TO mode activation by disorder.[20,21] For $x>0.2$ it decreases abruptly with Ge concentration because the alloy loses its polar character as Ge atoms occupy Ga and As atomic sites, so TO mode has to decrease as less Ga and As atoms are present in the alloy. Although there is an abrupt decrease of the ratio in the range $0.2 \leqslant x \leqslant 0.4$, the TO mode phonon is still present in alloys with Ge concentrations higher than 0.4. This has to be associated with the presence of zinc-blende domains in the whole compositional range that is predicted by the simulations and that has been experimentally observed for this kind of alloys.[22] The extrapolation to zero of this ratio for samples of all substrate orientation plotted in Fig. 7 provides a value for $x_c \approx 0.38$, a value similar to that obtained in Ref. 20 of $x_c \approx 0.35$ for (001)-oriented samples. The uncertainty in the extrapolation precludes us to ascertain if the small difference may be of any significance.

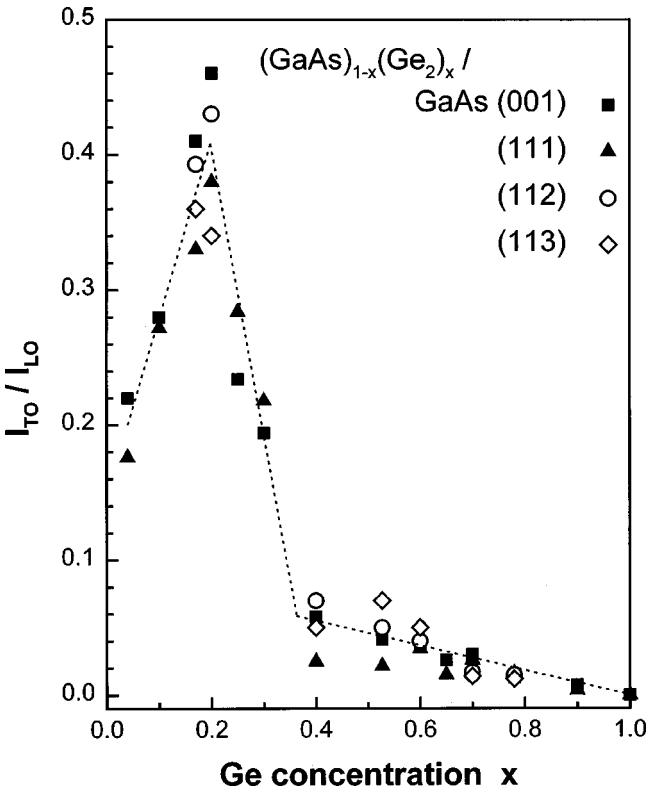

FIG. 7. Dependence on Ge concentration of the ratio of TO mode to LO mode integrated intensities of $(GaAs)_{1-x}(Ge_2)_x$ grown on different substrate orientations. The lines are for visual aid only.

The remarkable fact about the Raman scattering results is that it indicates that the short-range order is almost identical for all the substrate orientations examined. The behavior with Ge concentration of the SRO has an interesting shape but the maximum or minimum cannot be associated with an order disorder transition. Although in a macroscopic scale there is a critical concentration characteristic of each growth direction and the long-range order is ruled by the substrate geometry, the short-range order is independent of the substrate orientation. The density of the different atomic pairs (Ga-Ge, Ga-As, As-Ge, Ge-Ge) is the same for the different substrate orientations for a given Ge concentration, which leads to a very similar SRO. However it is the different arrangement of this pairs (ruled by the geometry), which in a macroscopic scale leads to a different LRO.

C. Absorption measurements

The optical gaps were obtained fitting the absorption spectra of the samples to the relationship $(\alpha h\nu)^{1/2} = A(h\nu - E_0)$ where α is the optical absorption coefficient and A is a

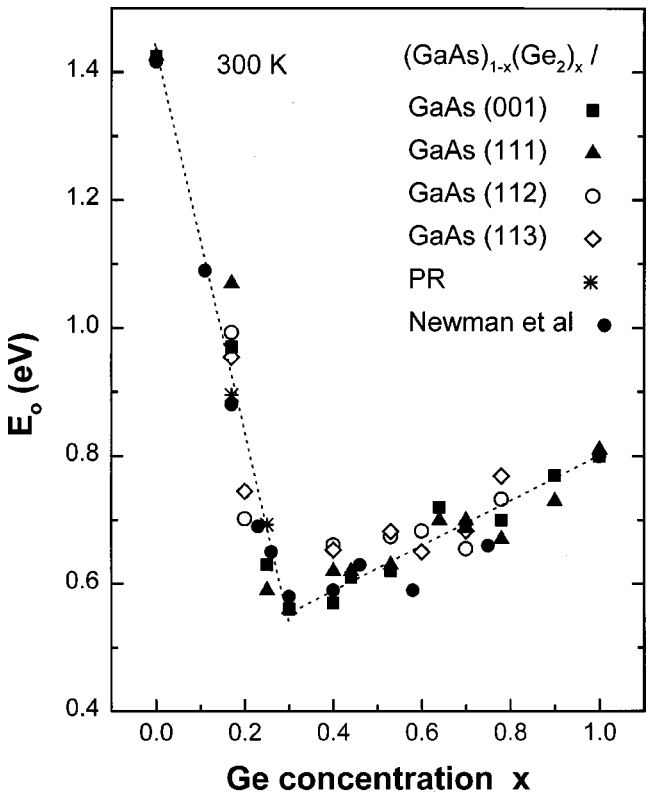

FIG. 8. Optical gap behavior with Ge concentration measured at room temperature for $(GaAs)_{1-x}(Ge_2)_x$ on (001), (113), (112), and (111) GaAs. The minimum observed near $x=0.3$ cannot be associated with the long-range order-disorder transition. The dashed lines are fits to two linear expressions $E_0(x)=1.43-2.99x$ eV and $E_0(x)=0.45+0.35x$ eV for $0<x<0.3$ and $0.3<x<1$. respectively, that show the behavior of the optical gap.

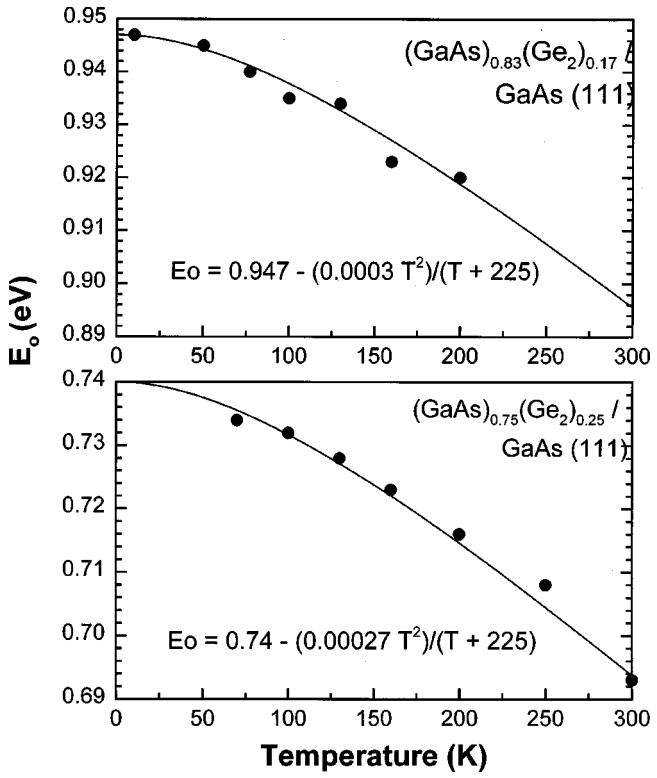

FIG. 9. Temperature dependence of the optical gap, E_0 of $(GaAs)_{0.83}(Ge_2)_{0.17}$ and $(GaAs)_{0.75}(Ge_2)_{0.25}$ alloys grown on (111) GaAs. The values for E_0 were obtained from the photoreflectance spectra fitting the curves to line shapes for a band to band transition.

fitting parameter. This expression is commonly used to determine the optical gap of materials, where selection rules are relaxed and where simple parabolic bands are assumed.[23] Measured optical gaps are shown in Fig. 8 as a function of the Ge concentration for (001)-, (113)-, (112)-, and (111)-grown alloys. It can be observed that all sets of alloys show a very similar gap behavior, moreover the V-shaped bowing previously reported (solid circles)[1] is also exhibited by our alloys. However, as we have shown that (111) alloys do not suffer an order-disorder transition at any Ge concentration, the minimum in the optical gap around $x=0.3$ *cannot* be associated with the long-range order disorder transition exhibited by (001)-grown alloys. Since the energy gap of these alloys is dominated by the short-range order these results only reconfirm what was observed by Raman scattering, i.e., that SRO is independent of substrate orientation.

The dashed lines in Fig. 8 are fits to the experimental data with linear functions that show the optical gap behavior with Ge concentration of these alloys at room temperature. For $0<x<0.3$ and $0.3<x<1$ the empirical expressions are $E_0(x)=1.43-2.99x$ eV and $E_0(x)=0.45+0.35x$ eV, respectively.

D. Photoreflectance measurements

Only for two (111)-grown alloys (those with $x=0.17$ and 0.25) was it possible to obtain a photoreflectance signal. The values for E_0 as a function of temperature were obtained fitting the PR spectra using the theory developed by Aspnes[24] for electroreflectance, taking the line shape in the low-field limit for a band to band transition. The behavior with temperature of the fitted energy values for E_0 are shown in Fig. 9 for both the samples. The solid lines are fits to the empirical expression developed by Varshni[25] that describes the dependence with temperature of the energy gaps of group-IV and -III-V cubic semiconductors, $E(T)=E(0)-AT^2/(T+\Theta)$, where Θ is the Debye temperature and A is a fitting parameter. In our fits Θ was fixed to 225 K, the Debye temperature of GaAs, in order to reduce the fitting to two parameters A and $E(0)$. We are also justified in making this choice because the Debye temperatures of both Ge and GaAs are expected to be very similar. The variation of Θ up to 300 K has minimum effect on the values of E_0 (changes of the order of the experimental uncertainty of E_0) at least in the studied temperature range, that result in $E_0(0)=0.947$ and 0.740 eV, and $A=3\times10^{-4}$ and 2.7×10^{-4} eV/K, for samples of $x=0.17$ and 0.25, respectively. The overall uncertainty is within ±0.003 eV at 10 K and ±0.007 eV at 300 K. The values obtained for A and $E(0)$ are shown in the Varshni formula in Fig. 9 for both samples. The energy gaps from PR spectra at room temperature are shown by stars in Fig. 8. The value of the energy gap for the sample with $x=0.17$ at room temperature was obtained from extrapolation to 0 K using the fit. The values for the optical gap from PR are in reasonable agreement with those from optical absorp-

tion, but the former are more precise. PR was intended for many other samples, but in those the number of defects seems to be so high that the Fermi energy at the sample surface is pinned to some fixed value producing bands that are difficult to modulate by the photogeneration of new carriers.

VI. FINAL COMMENTS AND CONCLUDING REMARKS

$(GaAs)_{1-x}(Ge_2)_x$ metastable alloys were epitaxially grown on (001), (111), (112), and (113) GaAs by rf magnetron sputtering. Long-range order parameter for these alloys was determined from fundamental and superstructure reflections obtained by HRXRD. A different order parameter behavior with Ge concentration is observed for each growth direction. From experimental data we obtain a critical concentration characteristic of each substrate orientation. This provides a direct evidence that growth direction affects the long-range order-disorder transition exhibited by these alloys. From Raman scattering and optical absorption we observe that the ratio l_{TO}/l_{LO} and the fundamental gap are very similar for all the substrate orientations so the special features as the band gap minimum at $x \approx 0.3$ cannot be associated with an order-disorder transition. The optical properties are governed almost entirely by nearest neighbor atomic interactions, i.e., the short-range order.

We modeled the epitaxial growth of these alloys for (001)-, (111)-, (112)-, (113)-, and (110)-oriented growth. The good agreement between the experimental and modeled long-range order parameter evidences that atomic ordering in these alloys is ruled mainly by the substrate geometry and the sticking coefficients among the constituent atoms (Ga-Ga and As-As equals to zero), rather than by the minimization of any thermodynamical potential.

ACKNOWLEDGMENTS

The authors acknowledge the financial support of Consejo Nacional de Ciencia y Tecnologia (CONACYT), Mexico, and from FAI-UASLP, during the course of this research.

[1] Kathie E. Newman, A. Lastras-Martinez, B. Kramer, S. A. Barnett, M. A. Ray, J. D. Dow, J. E. Greene, and P. M. Raccah, Phys. Rev. Lett. **50**, 1466 (1983).
[2] S. I. Shah, B. Kramer, S. A. Barnett, and J. E. Greene, J. Appl. Phys. **59**, 1482 (1986).
[3] Zh. I. Alferov, M. Z. Zhingarev, S. G. Konnikov, I. I. Mokan, V. P. Ulin, V. E. Umanskii, and B. S. Yavich, Fiz. Tekh. Poluprovodn. **16**, 831 (1982) [Sov. Phys. Semicond. **16**, 532 (1982)].
[4] D. H. Mei, Y. W. Kim, D. Lubben, I. M. Robertson, and J. E. Greene, Appl. Phys. Lett. **55**, 2649 (1989).
[5] B. Salazar-Hernández, M. A. Vidal, M. E. Constantino, H. Navarro-Contreras, and R. Asomoza, J. Cryst. Growth **197**, 783 (1999).
[6] A. G. Norman, J. M. Olson, J. F. Geisz, H. R. Moutinho, A. Mason, M. M. Al-Jassim, and S. M. Vernon, Appl. Phys. Lett. **74**, 1382 (1999).
[7] B. L. Gu, K. E. Newman, and P. A. Fedders, Phys. Rev. B **35**, 9135 (1987).
[8] R. J. Baird, H. Holloway, M. A. Tamor, M. D. Hurley, and W. C. Vassell, J. Appl. Phys. **69**, 226 (1991).
[9] A. G. Rodriguez, H. Navarro-Contreras, and M. A. Vidal, Microelectron. J. **31**, 439 (2000); Appl. Phys. Lett. **77**, 2497 (2000).
[10] Kathie E. Newman and John D. Dow, Phys. Rev. B **27**, 7495 (1983).
[11] Kyungha Kim and Edward A. Stern, Phys. Rev. B **32**, 1019 (1985).
[12] L. C. Davis and H. Holloway, Phys. Rev. B **35**, 2767 (1987).
[13] H. Holloway and L. C. Davis, Phys. Rev. B **35**, 3823 (1987).
[14] E. A. Stern, F. Ellis, K. Kim, L. Romano, S. I. Shah, and J. E. Greene, Phys. Rev. Lett. **54**, 905 (1985).
[15] M. I. Dyakonov and M. E. Ralkh, Fiz. Tekh. Poluprovodn. **16**, 840 (1982) [Sov. Phys. Semicond. **16**, 570 (1982)].
[16] H. Holloway and L. C. Davis, Phys. Rev. Lett. **53**, 830 (1984).
[17] B. E. Warren, *X-Ray Diffraction* (Dover, MA, 1992).
[18] A. Lastras-Martinez, G. Rodriguez-Pedroza, D. H. Mei, B. Kramer, D. Lubben, and J. E. Greene, Phys. Rev. B **43**, 14 035 (1991).
[19] Peter Y. Yu and M. Cardona, *Fundamentals of Semiconductors* (Springer, Berlin, 1996).
[20] B. Salazar-Hernández, M. A. Vidal, M. E. Constantino, and H. Navarro Contreras, Solid State Commun. **109**, 295 (1999).
[21] D. Olego and M. Cardona, Phys. Rev. B **24**, 7217 (1981).
[22] T. C. McGlinn, M. V. Klein, L. T. Romano, and J. E. Greene, Phys. Rev. B **38**, 3362 (1988).
[23] J. Pankove, *Optical Processes in Semiconductors* (Dover, NY, 1971).
[24] D. E. Aspnes and A. A. Stunda, Phys. Rev. B **7**, 4605 (1973).
[25] Y. P. Varshni, Physica (Amsterdam) **34**, 149 (1967).